Ferroelectrics, 1982, Vol. 45, pp. 1–12
0015-0193/82/4501-0001/$06.50/0

PHOTOGALVANIC EFFECTS INVESTIGATION IN GALLIUM ARSENIDE

V. L. ALPEROVICH, V. I. BELINICHER, V. N. NOVIKOV and A. S. TEREKHOV

Institute of Semiconductor Physics, Institute of Automation and Electrometry, Siberian Branch, USSR Academy of Sciences, 630090, Novosibirsk 90, USSR

(*Received June 3, 1981*)

A theory of the bulk photogalvanic effect, surface photogalvanic effect, photon drag effect for optical interband transitions in gallium arsenide is constructed. These effects are experimentally discovered and investigated. The magnetic field action and the surface photogalvanic effect is studied theoretically and experimentally. The quantitative agreement between the theory and experiment is obtained.

1. INTRODUCTION

The phenomena consisting in the current appearance in crystals due to the light absorption at the expense of drift and diffusion of photoinduced electrons and holes are called photoelectric.[1] A new class of the photoelectric phenomena, where photocurrents appear in the external field and concentration gradient absence has been studied actively in the last few years. The photocurrent nature is caused not by the drift and diffusion processes of electrons and holes, but it has origin in the process of free ballistic motion during the momentum relaxation time after the photoexcitement process. It is natural to call the photocurrents of that nature as ballistic photocurrents.

The oriented motion of the current carriers has origin in the momentum distribution asymmetry at the moment of photoexcitation, i.e. due to dominant generation of electrons and holes in a definite direction. The photocurrents of that nature can arise not only due to asymmetry in photoexcitation act but also due to anisotropy in the momentum distribution, spin polarization and hot electron (hole) distribution function difference from equilibrium distribution function. The photocurrent arises in those cases due to electron and hole scattering processes asymmetry. For the ballistic photocurrent appearance in the system crystal plus light the symmetry center must absent or, more definitely, the direction must be distinguished, which can be characterized by polar vector. This class of phenomena includes the photogalvanic effect in noncentrosymmetric media (PGE),[2,3] photon drag effect of electrons and holes (PDE),[4] surface photogalvanic effect (SPG)[5,6] anisotropic photoconductivity (APC),[7] reactive photoemf,[8] resonance photocurrent.[9] We shall call all those effects as photogalvanic effect and emphasize that the nature of these effects is caused by the center symmetry absence in the system crystal plus light and it is not connected with external fields and the current carriers concentration gradients. The nonthermalized electrons and holes make usually dominant contribution in photogalvanic effects. The energy of nonthermalized charge carriers is fixed by the conservation low in the photoexcitation act. The free path length of nonthermalized electrons (holes) $\Lambda(E_0)$ differs essentially from the free path length of the thermalized electrons and holes $\Lambda(T)$ and it depends essentially on the energy E_0. The photogalvanic effect investigation gives unique possibility of direct definition of $\Lambda(E_0)$ and also band structure parameters which have influence on the photogalvanic effects.

The interband optical transitions in gallium arsenide give the possibility to construct the quantitative theory of the photogalvanic effects. The results of theoretical calculations are expressed through a small number of constants that are crystal characteristics and are known from independent experiments. Good quality of GaAs crystals gives possibility to produce precise experiments and perform the comparison between theoretical calculations and experimental results. The photogalvanic effects investigated in the present paper are defined by the following phenome-

nological relations that give the relation between the photocurrent **j**, light intensity I and its polarization vector **e**:

$$j_i = I\beta(\omega)\,|\epsilon_{ijl}|e_j e_l^* \tag{1}$$

is photogalvanic effect in noncentrosymmetrical media (ϵ_{ijl} is a unique antisymmetrical tensor);

$$j_i = I\gamma(\omega)[(e_i - n_i(\mathbf{en}))(\mathbf{e}^*\mathbf{n}) + \text{h.c.}] + iI\delta(\omega)[\mathbf{n} \times [\mathbf{e} \times \mathbf{e}^*]]_i \tag{2}$$

is surface photogalvanic effect (**n** is a normal vector)†

$$j_i = \alpha(\omega) q_i I \tag{3}$$

is photon drag effect (**q**, ω are momentum and frequency of light). These three effects can be separated by characteristic dependence on the orientation of crystal axes orientation about its surface, angles between the direction of light propagation and normal vector **n** and also crystal axes, the direction of the light polarization vector, the direction of the current propagation. The magnetic field effectively turns the photocurrents (1)–(3) and the terms that have the structure $[\mathbf{H} \times \mathbf{j}]$ appear in phenomenological relations (1)–(3), where **j** is photocurrent in the magnetic field absence.

2. THE THEORY OF PHOTOGALVANIC EFFECTS FOR INTERBAND TRANSITIONS IN GaAs

It is necessary to find the probability of electron and hold photogeneration $W_{\mathbf{k}}$ for calculation of photogalvanic effects. For this SPG is defined by the anisotropic part of $W_{\mathbf{k}}$ that is proportional to $|\mathbf{ke}|^2$;‡ PGE is defined by antisymmetrical with respect to momentum **k** parts $W_{\mathbf{k}}^{as} = -W_{-\mathbf{k}}^{as}$, which is not connected with photon momentum $W_{\mathbf{k}}^{as} \sim |\epsilon_{ijl}|k_i e_j e_l$;[2] PDE is defined by the asymmetrical part of electron and hole photogeneration probability proportional to photon momentum **q**: $W_{\mathbf{k}} \sim (\mathbf{k} \cdot \mathbf{q})$.

The electron and hole probability of photogeneration in the channel ν with momentum $\mathbf{k}_e$, $\mathbf{k}_h$ can be written in the following manner:

$$W^{\nu}_{\mathbf{k}_e\mathbf{k}_h} = \frac{I}{2\pi c} \sum_{\alpha,\beta=\pm 1/2} \times |D_{\alpha,\nu\beta}(\mathbf{k}_e, \mathbf{k}_h)\mathbf{e}|^2 \delta(\epsilon^e_{\mathbf{k}_e} + \epsilon^{h\nu}_{\mathbf{k}_h} + E_g - \hbar\omega) \tag{4}$$

Here $\mathbf{k}_e + \mathbf{k}_h = \mathbf{q}$, $\mathbf{D}_{\alpha,\nu\beta}(\mathbf{k}_e, \mathbf{k}_h)$ is matrix element of dipole momentum between the hole state $|\nu\beta\mathbf{k}_h\rangle$ and electron state $|\alpha, \mathbf{k}_e\rangle$, $\epsilon^e_{\mathbf{k}}$, $\epsilon^{h\nu}_{\mathbf{k}}$ are dispersion laws of the electron and ν hole. This matrix element **D** is defined by the wave functions in the Keine theory which is described by the following Hamiltonian[11]

$$\mathcal{H} = \begin{pmatrix} Rk^2 + E_g, & iPk_i + \lambda\,|\epsilon_{ijl}|k_j k_l/2 \\ \text{h.c.}, & -Mk^2\delta_{ij} - \Lambda k_i k_j - \Delta\sigma_i\sigma_j \end{pmatrix} \tag{5}$$

Here the upper block is a 2×2 matrix and it corresponds to s bands; the lower block is a 6×6 matrix and it corresponds to p bands; the p band wave functions are numerated by vector indices $i, j = 1, 2, 3$; σ_i are Pauli matrices; R, M, $\Lambda = L - M$, P are standard parameters of the Keine theory. The spectrum of the Hamiltonian is shown in Figure 1. Note, that the goffer effects give a correction less than ten percent with respect to isotropic ef-

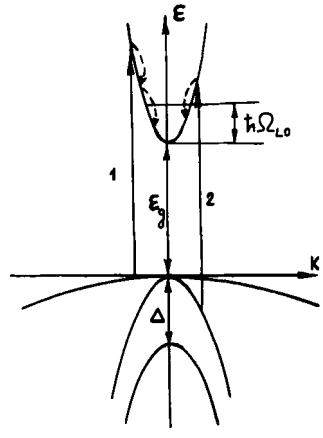

FIGURE 1 The band GaAs structure. Horizontal lines in the conducting band limit the electron passive band. 1 and 2 are the interband transitions from the bands of heavy and light holes respectively. The dotted lines mark thermalization processes with the optical phonons emission.

† APC in GaAs is defined by the phenomenological relation which coincides by the form with Eq. (2) if normal vector **n** is changed by the external electric field **E**. The APC theory which is applicable to electrons in GaAs was developed in paper referred to in Ref. 10.

‡ The term $|\mathbf{ke}|^2$ in $W_{\mathbf{k}}$ defines the linear SPG [the constant $\gamma(\omega)$ in relation (2)], circular SPG [the constant $\delta(\omega)$ in relation (2)] on the interband transitions in GaAs is caused by the photoelectron spin polarization. The theory of this effect applicable to electrons in GaAs was developed in the paper referred to in Ref. 13.

fects. By the $W^{\nu}_{\mathbf{k}_e,\mathbf{k}_h}$ probability calculation it is sufficient to know the projection operators on the hole wave functions $u^{\nu\beta}_{\mathbf{k}i\alpha}$ is not essential for the hole wave functions $u^{\nu\beta}_{\mathbf{k}i\alpha}$ is not essentional for the final formula. The projection operators are defined by the following relations:

$$\Pi^{\nu}_{i'\alpha',i\alpha} = \sum_{\beta=\pm 1/2} u^{\nu\beta}_{\mathbf{k}i'\alpha'} u^{\nu\beta*}_{\mathbf{k}i\alpha} \tag{6}$$

The effective method of projection operators (6) obtaining was developed in Ref. 14. This method gives a possibility to find also spectrum Hamiltonian (5). This method is based on the Green function of Hamiltonian (5) that has the form:

$$G(E,\mathbf{k}) = \sum_{\nu=\pm 1,0} \Pi^{\nu}(\mathbf{k})/(E - \epsilon^{\nu}_{\mathbf{k}} - i\delta) \tag{7}$$

Here $\nu = \pm 1$ for light and heavy holes and $\nu = 0$ for splitted holes. Explicit form of the projection operators $\Pi^{\nu}_{\mathbf{k}}$ in the Keine theory was obtained in the paper referred to in Ref. 14. These projection operators reduce difficult calculations with the hole wave functions.

For obtaining the quantative results for the photogalvanic effects in gallium arsenide it is necessary to take into account the Coulomb electron hole interaction. The interaction was taken into account on the base of the following integral equation for the matrix element of the dipole momentum **D**:

$$(D_{\alpha,\nu\beta}(\mathbf{k}_e,\mathbf{k}_h))_l = \frac{ieP}{\omega} F^{\nu}_{i\alpha,j\gamma}(\mathbf{k}_e,\mathbf{k}_h)\, u^{\nu\beta}_{\mathbf{k}_h j\gamma} \tag{8}$$

here dynamical factor of the dipole momentum $F^{\nu}_{\alpha,j\gamma}(\mathbf{k}_e,\mathbf{k}_h)$ satisfies the integral equation:

$$\int\Bigg[\delta_{il}\delta(\mathbf{p}) + \frac{e^2}{2\pi^2\epsilon_0\mathbf{p}^2}\sum_{\nu=\pm 1,0}\frac{\Pi^{\nu}_{il}(\mathbf{k}_h - \mathbf{p}/2)}{\epsilon^{e}_{\mathbf{k}_e} + \epsilon^{h\nu}_{\mathbf{k}_h} - \epsilon^{e}_{\mathbf{k};\mathbf{p}/2} - \epsilon^{h\nu}_{\mathbf{k}_h-\mathbf{p}/2} - i\delta} \times F^{\nu}_{lj}\left(\mathbf{k}_e + \frac{\mathbf{p}}{2}, \mathbf{k}_h - \frac{\mathbf{p}}{2}\right)d\mathbf{p} = \delta_{ij} - i\lambda\,|\epsilon_{ijl}|(k_e - k_h)_l/2P$$

here ϵ_0 is static dielectric permittivity, e is electric charge. The dynamical factor $F^{\nu}_{ij}(\mathbf{k}_e,\mathbf{k}_h)$ can be found if one uses the fact of dependence $F^{\nu}_{ij}(\mathbf{k}_e,\mathbf{k}_h)$ from relative momentum $\mathbf{k} = (\mathbf{k}_e - \mathbf{k}_h)/2$ in the center mass system and its independence from $\mathbf{k}_e$, $\mathbf{k}_h$ separately. This fact is based on the small parameter $(\mu_h - \mu_e)/(\mu_h + \mu_e) \approx 0.2$ here μ_h, μ_e are reduced masses of an electron and heavy or light hole. Using the solution of a usual Coulomb problem one can obtain:

$$F^{\nu}_{ij}(\mathbf{k}) = \left(\delta_{ij} - i\frac{\lambda}{P}|\epsilon_{iln}|k_n\right)\frac{\sigma_l\sigma_j}{3} + \exp\left(\frac{f}{2}\right) \times \left(\Gamma(1+if)\delta_{il} - i\frac{\lambda}{P}\Gamma(2+if)|\epsilon_{iln}|k_n\right)\left(\delta_{lj} - \frac{\sigma_l\sigma_j}{3}\right) \tag{9}$$

Here $f = 1/ka_{\nu}$, a_{ν} is Bohr radius of the electron-hole system. From Eqs. (4) and (9) one can obtain an explicit form for photogeneration electron and hole probability $W^{\nu}_{\mathbf{k}}$ in the center mass system:

$$W^{\nu}_{\mathbf{k}} = \frac{3\kappa_{\nu}I}{32\pi\hbar\omega}\frac{\eta_{\nu}}{k\mu_{\nu}}\delta(\epsilon^{\nu}_{\mathbf{k}} + E_g - \hbar\omega) \tag{10}$$

Here $\epsilon^{\nu}_{\mathbf{k}} = k^2/2m_e + \epsilon^{h\nu}_{\mathbf{k}}$, $\epsilon^{hh}_{\mathbf{k}} = Mk^2$, $\epsilon^{hl}_{\mathbf{k}} = (M - \Lambda/2)k^2 + (\Delta - D)/2$ the dimensionless quantity $\eta_{\nu} = \eta^{s}_{\nu} + \eta^{as}_{\nu}$ has the form $\eta^{s}_{\nu} = 3 - \nu + (1+\nu)\cos\psi(\tilde{k}) - |\tilde{\mathbf{k}}\mathbf{e}|^2/\tilde{\mathbf{k}}^2[1 - 3\nu + 3(1+\nu)\cos\psi(\tilde{k})]$, $\eta^{as}_{\nu} = 8\lambda\,|\epsilon_{ijl}|k_i e_j e_l/15\ Pka_{\nu}$, $\cos\psi(k) = -(\Delta - 3\Lambda k^2)/3D$, $D = (\Delta^2 - 2\Lambda k^2\Delta/3 + \Lambda^2k^4)^{1/2}$, $\tilde{\mathbf{k}} = \mathbf{k} \pm \mu_{\nu}\mathbf{q}/m_e$ for electron and hole, excitation respectively, κ_{ν} is partial absorption coefficient that includes the Coulomb interaction effects

$$\kappa_{\nu} = \frac{4}{3}\frac{e^2}{\hbar c}\frac{\mu_{\nu}k_{\nu}P^2}{\hbar^3\omega n_{\omega}}|Z_{k\nu}|^2$$

where n_{ω} is a refractive index, $Z_{k\nu}$ is Zommerfeld factor:

$$|Z_{k\nu}|^2 = f\cdot(1 - \exp(-f))^{-1};\quad \kappa = \kappa_{+} + \kappa_{-}$$

The probability of electron and hole generation $W^{\nu}_{\mathbf{k}}$ can be used directly for calculation of PGE, SPG, PDE. The probability was calculated also from the perturbation theory for electron-hole interaction, for this the band structure of GaAs was precisely taken into account in approximation $\Delta/E_g \ll 1$, i.e. the mixing light and splitting holes and also nonparabolic form of the light hole band was taken into account. We did not give the corresponding formula because they are very complicated.[14] On the basis of formula (10) one can easily calculate the photocurrent:

$$\mathbf{j} = e\sum_{\nu}\int W^{\nu}_{\mathbf{k}}\left(\frac{\partial\epsilon^{e}_{\mathbf{k}'}}{\partial\mathbf{k}'}\Gamma^{-1}_{e\mathbf{k}'} - \frac{\partial\epsilon^{h\nu}_{\mathbf{k}''}}{\partial\mathbf{k}''}\Gamma^{-1}_{h\nu\mathbf{k}''}\right)d\mathbf{k} \tag{11}$$

Here Γ_{ek}, $\Gamma_{h\nu k}$ are frequencies of momentum relaxation for electron and ν hole, $\mathbf{k}' = \mathbf{k} + \mu_\nu/m_{h\nu}\,\mathbf{q}$, $\mathbf{k}'' = \mathbf{k} + \mu_\nu/m_e\,\mathbf{q}$. Formula (11) is valid if the electron or hole kinetic energy does not exceed the optic phonon energy $\hbar\Omega_{LO} = 0.037$ ev. In that case the electron and hole are in the passive band, and Γ_{ek}, $\Gamma_{h\nu k}$ at low temperature form due to the scattering on the impurity and acoustic phonons. For ϵ_k^e, $\epsilon_k^{h\nu} > \hbar\Omega_{LO}$ the momentum relaxation is produced by two steps. The photoelectrons and holes emit quickly one or several optical phonons and transit in the passive band. Partial decreasing of asymmetry and anisotropy of the photogeneration probability takes place. The process of isotropization is completed due to scattering processes in the passive band. The basic characteristic of the isotropization process by the optical phonon emission is the isotropy function $U_L(\epsilon)$ defined as a relation of the coefficients in decomposition generation function with respect to spherical functions $\Upsilon_{LM}(\theta, \varphi)$ by the energy in the passive band $\tilde{\epsilon} = \epsilon - \hbar\Omega_{LO}$ Int $(\epsilon/\hbar\Omega_{LO})$ to that coefficients in the active band at the energy of the photoexcitation ϵ. An explicit form of isotropy functions $U_L(\epsilon)$ can be found if we solve balance equations for distribution function of the photoelectrons and holes for the energy $\epsilon_p = \epsilon - p\hbar\Omega_{LO}$, $p = 0, 1, \ldots, n = \text{Int}\,(\epsilon/\hbar\Omega_{LO})$. These functions have the following form:

$$U_L^e(\epsilon) = \prod_{p=1}^{n} Q_L(q_p)/Q_0(q_p)$$

for electrons. Here $q_p = (k_p^2 + k_{p-1}^2)/2k_pk_{p-1}$, $k_p^2 = 2m(\epsilon - p\hbar\Omega_{LO})$, $Q_L(x)$ is the Legandre function of the second type.

$$U_{L\nu'\nu}^h = \left(\prod_{p=1}^{n} Z_{Lp}\right)_{\nu'\nu} \tag{12}$$

for holes. Here $\nu = 1$ for light holes, $\nu = -1$ for heavy holes and 2×2 matrix $(Z_{Lp})_{\nu'\nu}$ is a linear combination of the functions similar to $Q_L(x)$. An explicit form of these functions is given in the paper referred to in Ref. 6. The electron isotropization function is presented in Figure 2. For $L = 2$ this function has been first obtained in the paper referred to in Ref. 15. PDE, PGE are essentially defined by isotropy function at $L = 2$. The probability of the appearance of electrons and holes in the passive band follows from probability (10) with the help of the isotropy functions $U_L^e(\epsilon)$, $U_{L\nu'\nu}^{h\nu}(\epsilon)$. For electrons it is sufficient to multiply probability (10) by $U_L(\epsilon)$, for holes to multiply it by $U_{L\nu'\nu}^{h\nu}(\epsilon)$ and to make summation in two different channels of hole generation.

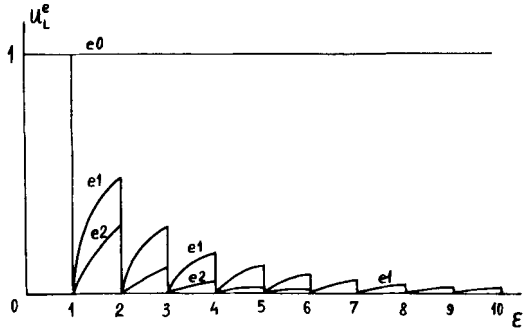

FIGURE 2 The electron isotropy functions $U_L^e(E)$ for $L = 0, 1, 2$. The energy E is measured at the optical phonon energy units. The function $U_L^e(\epsilon)$ graphs are shown with symbols eL.

On the basis of Eq. (11) for PDE and PGE and using known expressions for photocurrent in the frameworks of kinetik theory[5,6] one can obtain a final expression for the photocurrent. The constant $\gamma(\omega)$ for surface photogalvanic effect has the form:

$$\gamma(\omega) = \frac{e}{8\hbar\omega} \sum_{\nu'\nu} (3\nu - 1 - 3(1+\nu)\cos\psi)\frac{\kappa_\nu}{\kappa} \times [P_e \Lambda_\nu^e U_2^e(\epsilon_\nu^e) \times f(\kappa\Lambda_\nu^e) - P_{h\nu}\Lambda_\nu^h U_{2\nu'\nu}^h(\epsilon_\nu^h) f(\kappa\Lambda_{\nu'}^h)]; \quad f(x^{-1}) = \frac{1}{8}\left[12x^2(1-x^2)\ln\frac{1+x}{x} + 3 - 8x - 6x^2 + 12x^3\right] \tag{13}$$

here P_e, $P_{h\nu}$ are diffusion coefficients for electrons and holes. The photogalvanic effect is determined by the constant $\beta(\omega)$:

$$\beta(\omega) = \frac{2e}{15\hbar\omega} \sum_{\nu',\nu} \frac{\kappa_\nu}{\kappa}\frac{\lambda}{a_\nu P} \times (10 + \nu)[\Lambda_\nu^e U_1^e(\epsilon_\nu^e)\delta_{\nu'\nu} + \Lambda_\nu^h U_{1\nu'\nu}^h(\epsilon_\nu^h)] \tag{14}$$

The expression for the constant $\alpha(\omega)$ for photon drag effect is as follows:

$$\alpha(\omega) = \frac{2e}{5\hbar\omega} \sum_{\nu\nu'} \frac{\kappa_\nu}{\kappa}\left\{\delta_{\nu'\nu}\left[\Lambda_\nu^e U_1^e(\epsilon_\nu^e)\left(\frac{\mu_\nu}{m_{h\nu}}\tilde{\alpha}_\nu(\epsilon_\nu^e) + \beta(\epsilon_\nu^e) + \frac{\mu_\nu\epsilon_\nu^e}{m_{h\nu}}\tilde{\alpha}_\nu^2\frac{d}{d\epsilon}(\Lambda_e(\epsilon)U_1^e(\epsilon))/\tilde{\alpha}_\nu(\epsilon)\right)\Big|_{\epsilon=\epsilon_\nu^e}\right] - \frac{\mu_\nu}{m_e}\Lambda_\nu^h U_{1\nu'\nu}^h(\epsilon_\nu^h)\tilde{\alpha}(\epsilon_\nu^h) - \frac{\mu_\nu}{m_e}\epsilon_\nu^h\frac{d}{d\epsilon}[\Lambda_{h\nu}(\epsilon) \times U_{1\nu\nu}^h(\epsilon)\tilde{\alpha}_\nu(\epsilon)]|_{\epsilon=\epsilon_\nu^h}\right\}$$

here $\Lambda_\nu^e \equiv \Lambda_e(\tilde{\epsilon}_\nu^e)$, $\Lambda_\nu^h \equiv \Lambda_{h\nu}(\tilde{\epsilon}_\nu^h)$ are free path lengths for electrons and holes in the passive band, $\tilde{\alpha}_\nu = 2\alpha_\nu + 2$, $\beta_\nu = 2 - 2\alpha_\nu$, $\alpha_\nu(\epsilon) = 3 + \cos\psi(\epsilon) - \nu[1 - \cos\psi(\epsilon)]$. Expression (15) for PDE contains energy derivatives of the step function $\Lambda_e(\tilde{\epsilon})U_1^e(\epsilon)$, $\Lambda_\nu^h(\tilde{\epsilon})U_{1\nu'\nu}^h(\epsilon)$, which results in δ-function contribution to photocurrent. This effect of resonance recoil was considered theoretically in the papers referred to in Refs. 16 and 17 and spectra peculiarity connected with the effect of resonance recoil was observed in the experiments[18] for optical transitions between the bands of light and heavy holes in germanium. The form and width of the resonance recoil pick for interband optical transitions in gallium arsenide are defined by the finiteness of the photon momentum,[16] goffered form of the hole dispersion law,[17] and also by uniform broadening. The integral intensity of the resonance recoil picks is fixed by relation (15). For example, the integral intensity of the n-th pick in the series ν has the form:

$$Z_{\nu n} = \int j(\omega)d\omega$$

$$= \frac{2eI}{5\hbar\omega}\frac{q\kappa_\nu}{k_\nu\kappa} n\Omega_{LO}\frac{m_e}{m_{h\nu}}\tilde{\alpha}(n\Omega)n_e(\hbar\Omega_{LO})U_1^e(n\Omega - 0) \tag{16}$$

The constants $\alpha(\omega)$, $\beta(\omega)$, $\gamma(\omega)$ defined by relations (13), (14), (15) were calculated with a computer and the spectral curves were compared with the experimental data.

The theory of PDE, PGE and SPG was constructed at the presence of a uniform magnetic field. The influence of the magnetic field on PDE and PGE has the same character as in case of usual photoconductivity. For this the photocurrent $\mathbf{j}_H$ at the presence of the magnetic field is connected with the current $\mathbf{j}_0$ at the magnetic field absence by the relation:†

$$\mathbf{j}_H = \left(\mathbf{j}_0 - \frac{\Omega_c}{\Gamma}[\mathbf{h} \times \mathbf{j}_0]\right)/(1 + \Omega_c^2/\Gamma^2) \tag{17}$$

Here Ω_c is cyclotron frequency, Γ is collision frequency $\mathbf{h}$ is a unique vector along the magnetic field $\mathbf{H}$. In case of SPG the photocurrent change in the magnetic field is calculated in a more complicated manner because the magnetic field changes the character of electron scattering on the surface. Corresponding calculations were produced in the paper referred to in Ref. 10 and for the magnetic field which is normally oriented relative to the surface the photocurrent has the form:

$$j_x + ij_y = P\frac{\kappa_{aH}}{\kappa}\frac{eI}{\hbar\omega}\Lambda\left(1 - i\frac{\Omega_c}{\Gamma}\right)^{-1} f(\eta) \tag{18}$$

Here $\eta = \kappa\Lambda/(1 - i\Omega_c/\Gamma)$, x is current direction in the magnetic field absence; y is normally oriented direction along the surface, κ_{an}/κ is a relative part of anisotropically excited electrons. This expression for photocurrent is valid for electrons in the passive band of GaAs. For obtaining the electron photocurrent in the active band it is necessary to use the isotropy functions introduced above.

3. EXPERIMENTAL RESULTS AND COMPARISON WITH THE THEORY

We investigated experimentally:

a) surface photogalvanic effects caused by generation anisotropy of photoexcited electrons and their diffuse surface scattering;[6]

b) the magnetic field influence on the surface photogalvanic effect;

c) photon drag effect on interband optical transitions in which the resonance recoil by the electron optical phonon emission is observed;[19]

d) bulk photogalvanic effect connected with center symmetry absence in GaAs.

The measurements were performed on pure epitaxial n-GaAs layers with the mobility of $\mu \approx 10^5$ cm^2/v sec and concentration of $n \approx 2\cdot 10^{14}$ cm^{-3} at $T = 77$ K. Two electrodes in the form of parallel strips were put on the specimen surface by indium, as it was done for the photocundactivity measurements. For spectral dependence measurements an incandescent electric lamp and monochromator DFS-24 are used. Spectral resolution equals to $2\cdot 10^{-3}$ ev, intensity of incident and the specimen light was equal to $I = 10^{-5}$ wt/sm^2. The measurements are performed at the temperature of $T = 1.6 - 4.2$ K. The emf that arises under specimen illumination is experimentally measured. Polarization changes in the light intensity ab-

† It is supposed that the mechanisms of PGE and PDE connected exclusively with magnetic field are absent. An example of such PGE mechanism due to electron polarization in the conducting band by magnetic field when electrons are excited from paramagnetic impurities is given in the paper referred to in Ref. 2.

sorbed in the specimen were taken into account by the normalization by the value of photoconductivity.

a) *The Surface Photogalvanic Effect*

The photocurrent appearance can be most obviously explained by electron scattering on diffuse surface. Let us suppose that the electrons excited by the light are distributed along the eight sloped to the surface as Figure 3 shows. Then the electrons which move the right lose the momentum quicker due to the surface scattering than those moving to the left and scatter in the volume. As a result the electron stream directed to the left arises. For the mirror surface the stream equals to zero. Thus SPG appears as a result of combination of two effects: the photoexcitation anisotropy (optical drawing[20]) and diffusion of the surface electron scattering. The emf caused by SPG (V_{SPG}) was distinguished on the background emf due to photon drag effect V_{PDE}, emf connected with PGE V_{PGE} and emf on the crystal nonhomogeneous V_0 due to the characteristic dependence from the incident light beam angle θ and the angle φ between the incident plane and the light vector polarization which follows from Eq. (3). If the incident plane is perpendicular to contacts then $V_{SPG} \sim \cos^2 \varphi$ on it changes the sign as the sign of the incident angle θ changes. The experimental dependence SPG from θ and φ is in a good agreement with the theory.

The spectrum of the surface photogalvanic effect measured by the sloped light incidence ($\theta = 50°$) as the emf difference in permissible for SPG polarization (e || to incidence plate) and in forbidden polarization (e⊥ to incidence plate) is shown in Figure 4. The spectrum has the form of damped signchangable oscillations caused by the process of the emission of the optical phonons by the electrons in the active band. The similar spectra were obtained in all investigated specimens. Let us give the qualitative explanation of their forms. The four types of particles (electrons and holes from every channel) can give their contributions to SPG at the light frequency $E_g < \hbar\omega < E_g + \Delta$.

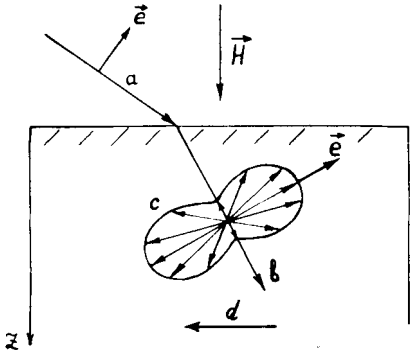

FIGURE 3 The obvious mechanism of the SPG formation (a) incident light beam, (b) refracted beam, (c) the angular photoelectron distribution, (d) the direction of the total electron stream; e is light vector polarization.

Let us consider the contribution of particles of a definite type, for example, electron from the heavy channel in the SPG spectrum. The spectrum form is connected directly with the dependence of the dominant momentum dissipation mechanisms from the energy. We supposed that the momentum dissipation on the charged impurities is dominated in GaAs at the helium temperatures for the electrons with kinetic energy less than the optical phonon energy $\hbar\Omega_{LO}$ (the passive band). So far as the free path length increases with the electron kinetic energy increase, the SPG increases with increase $\hbar\omega$. The fast emission of the longitudinal optical phonon by the electron takes place at the energy $\epsilon = \hbar\Omega_{LO}$. As a result, the total isotropization takes place and the uneven decrease of the SPG is observed. At the energy $\epsilon > \hbar\Omega_{LO}$ the partial isotropization of the electron distribution function takes place as a result of the optical phonon emission.[16] Thus the electrons spectrum from the heavy channel must consist of the damped oscillations connected with the electron emission of several optical phonons. The minimum energy of those oscillations can be described by the formula:

$$\hbar\omega_n = E_g + n\hbar\Omega_{LO}(m_e + m_h)/m_h \qquad (19)$$

here m_e, m_h are electron and heavy hole masses, n is integer number.

The form of the first oscillation is determined by the electron isotropization processes in the passive band. The form of the next oscillations both by those processes and the process of isotropization by the optical phonons emission. The electron contribution from the light channel has the opposite sign and the larger oscillation period. The largest period has the heavy hole contribution $\approx 9\hbar\Omega_{LO}$. The resulting SPG spectrum represents the sum of all four contributions and it should have the form of a signchangable damped oscillation. The experimentally measured spectra have just the same form. At the frequency $1.52 < \hbar\omega <$

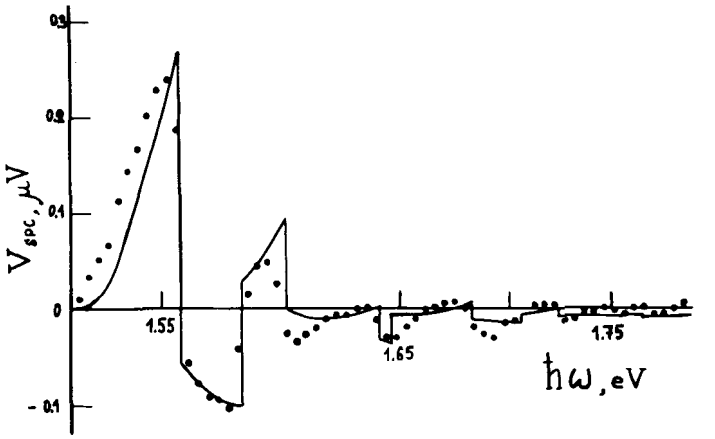

FIGURE 4 The SPG spectrum in a specimen S52 at the temperature $T = 4.2$ K°. The points mark the experimental results, represented with the spectrum dependence of the light intensity which comes out of the monochromator, the solid line represents the theoretical results.

1.56 ev the electron contribution from the heavy channel dominates at the frequency $\hbar\omega \sim 1.56$ ev these electrons emit a single optical phonon and the electron contribution from the light channel becomes dominated therefore V_{SPG} changes its sign and so on.

The theoretical spectrum calculated on computer on basis using Eq. (13) is represented in Figure 4 by a solid line. Evidently, that the theory describes well the thresholds of the phonons emissions and correlation of the oscillation amplitude. The diffusion coefficients for electrons and holes P_e, $P_{h\nu}$ are determined from the condition of the best fitting the theory and experiments considered, they are independent from the energy. The dependence of the diffusion coefficients on the energy can be determined from the experiments with magnetic fields (see below). The Keine Hamiltonian parameters are chosen on the basis of the known experimental data.[21] The free path length of the electrons and holes in the passive band were considered as caused by the scattering on the charged impurities with the concentration of $N = 5 \cdot 10^{14}$ cm^{-3} which was estimated according to the nitrogen mobility and also due to acoustic phonon emission.[10] The electron scattering on the surface was proved to be near the mirror: $P_e \simeq 0.2$. The hole contribution to SPG is essentially less than the electron contribution due to a stronger hole interaction with the acoustic phonons, therefore the corresponding diffusion coefficients can be approximately estimated as compared with P_e in the order of magnitude.

b) *Magnetic Field Action on Surface Photogalvanic Effect*†

The SPG spectra give the possibility to determine the energy dependence of the product of the diffusion coefficient on the free path length $V_{SPG} \sim P_e(E)\Lambda_e(E)$. The contribution of the bulk and surface scattering in SPG can be divided experimentally by measuring the dependence SPG on the magnetic field. Really, the magnetic field twists the photoelectron trajectories and thus turns the anisotropic part of the distribution function according to momentum[23,24] represented in Figure 3. In accordance with relations (17), (18) the change of V_{SPG} in the magnetic field is determined by the characteristic parameter Ω_c/Γ. If we find the parameter Ω_c/Γ then we determine the collision frequency according to the momentum Γ and, consequently, the free path length Λ_e. The magnetic field was directed perpendicularly to the specimen surface for the exception of the photoelectromagnetic Kikoin-Noskov effect. The magnitude of the V_{SPG} in the magnetic field was measured that for $\kappa\Lambda \gg 1$, as follows from Eq. (18), has the form:

$$V_{SPG}(H) = V_{SPG}(0)/(1 + \Omega_c^2/\Gamma^2) \qquad (20)$$

The dependence of the SPG on the magnetic field for two different photon frequencies in the

† The experimental results on the magnetic field action of PGE were obtained in cooperation with G. M. Gusev.

field of the first positive oscillation $\hbar\omega < 1.66$ ev is represented in Figure 6. Evidently, the SPG decreases in a rather small magnetic field of $H \sim 100$ g, moreover, the form of the SPG corresponds well to formulae (20) (a solid line in Figure 5). Note, that the anomalous strong action of the magnetic field on the PGE in $LiNbO_3$ and ZnS has been discovered recently in the papers referred to in Refs. 25 and 26. For the definite spectral point ω we determine the magnetic field $H_{1/2}$ where the SPG decreases two times. The free path length Λ as the function of the energy E was calculated on the basis of the dependence $H_{1/2}(\omega)$ (circles in Figure 6):

$$E = (\hbar\omega - E_g)m_h/(m_e + m_h) \qquad (21)$$

We neglected the contribution of the light channel electrons, that gives ≈20% contribution in the SPG in that spectral region. A solid line in Figure 6 represents the theoretical dependence of $\Lambda(E)$ with the account of the electron scattering on the charged impurities and deformational potential of the acoustic phonons:

$$\Lambda = (\Lambda_{im}^{-1} + \Lambda_{ac}^{-1})^{-1}$$
$$\Lambda_{im} = \epsilon_0^2 k^4 \hbar^4 / 4\pi N m_e^2 e^4 \ln(kr_s) \qquad (22)$$
$$\Lambda_{ac} = 5\pi\rho\hbar^3 c_s / 4\sigma_e^2 m_e^2 k$$

Here $\epsilon_0 = 12.5$ is the static dielectric permittivity; r_s is the screening radius $r_s = 10^{-5}$ cm; $\rho = 5.4$ g/cm^3 is GaAs density; $c_s = 5.2\ 10^5$ cm/sec is sound velocity. The charged impurity concentration N on the theoretical curve of Figure 6 was $3 \cdot 10^{14}$ cm^{-3}, and the constant of the deformation potential σ_e was 7 ev. The dotted line in Figure 6 corresponds to the scattering on the charged imparities only. It follows from Figure 6 that the free path length of the hot photoexcited electrons reaches the magnitude larger than 20 mcm, that exceeds the free path length of the thermalized electrons at the helium temperature by on 3–4 orders.

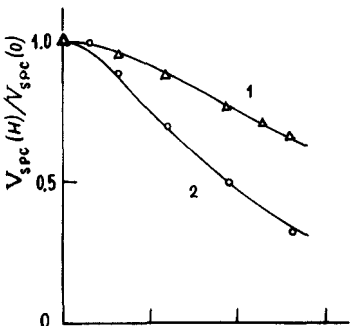

FIGURE 5 The SPG dependence on the magnetic field H at the light frequency of $\hbar\omega = 1.535$ ev (1) and at $\hbar\omega = 1.547$ ev (2). Which corresponds to the electron kinetic energy from the heavy channels of 14 mev and 25 mev (the specimen S33, $\mu \sim 10^5$ cm^2/v sec, $n \approx 1.5\ 10^{14}$ cm^{-3}).

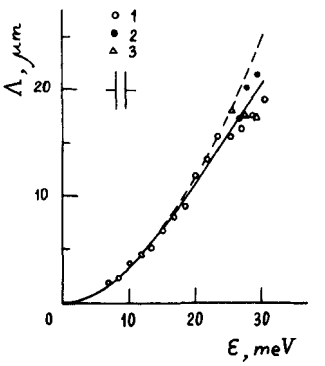

FIGURE 6 The dependence of free path length from the electron energy above the conducting band bottom. 1 and 2 represent electrons from heavy and light channel respectively, 3 represents the electrons from the heavy channel, excited in the active band $\hbar\Omega_{LO} < E < 2\hbar\Omega_{LO}$ (see the paper text). The solid line represents the free path length due to the scattering on the charged impurities and the acoustic phonons. A dotted line represents the free path length due to the scattering on the charged impurities only.

The dependence $V_{SPG}(H)$ was measured also in the spectral region of 1.56 ev $< \hbar\omega <$ 1.59 ev (the first negative oscillation) where the contribution in SPG of the electrons from the light channel is dominating. In Figure 6 the free path length of those electrons determined from the magnitude $H_{1/2}(\omega)$ is shown by dark circles. A good coincidence of the Λ magnitudes for the electrons from two different channels is obvious.

The free path length of the electrons excited by the light with the energy of $\hbar\Omega_{LO} < E < 2\hbar\Omega_{LO}$ determined according to the field $H_{1/2}$ must coincide with the free path length of the electrons excited explicitly in the passive band with the energy of $\bar{E} = E - \hbar\Omega_{LO}$, so far as the basic contribution in the photocurrent gives the electrons in the passive band after the optical phonon emission. This statement we verified experimentally by measuring the dependence $V_{SPG}(H)$ in the frequency region of 1.59 ev $< \hbar\omega <$ 1.615 ev (the second posi-

tive oscillation) where the basic contribution in the photocurrent is given by the electrons from the heavy channel that can emit a single optical phonon.

The experimental values of Λ for such electrons are shown with the triangles in Figure 6. The energy $\tilde{E} = E - \hbar\Omega_{LO}$ is noted along the horizontal axis. In the limits of the accidental error the Λ values for electrons in the active region with the energy $\tilde{E}$ coincide with Λ values in the passive region with the energy E. A similar picture should be observed for the electrons emitting two or more LO-phonons. It is difficult to verify this statement experimentally due to small SPG value at the light frequency of $\hbar\omega > 1.65$ ev. The magnitude of the electron contribution to the SPG from ballistic motion before the LO-phonon emission is out of the experimental precision limits.

The dependence of the diffusion coefficient $P(E)$ for the surface scattering from the energy E was obtained from the SPG spectrum $V_{SPG}(E)$ and the dependence $\Lambda(E)$ in the passive region: $P(E) \sim V_{SPG}/\Lambda(E)$ (Figure 7). Evidently, $P_e(E)$ decreases as E increases, and at the energy $E > 15$ mev the saturation takes place. The solid line was calculated according to the formula:

$$P_e(E) = P_0 + P_1/E^2 \qquad (23)$$

here $P_0 = 0.1$, $P_1 = 22$ mev^2. The term P_1/E^2 in formula (23) corresponds to the scattering on the surface centers with the concentration of $N_s = 2 \cdot 10^{10}$ cm^{-2}. The term P_0 independent on E is connected apparently, with the electron scattering on the neutral defects and surface roughness.

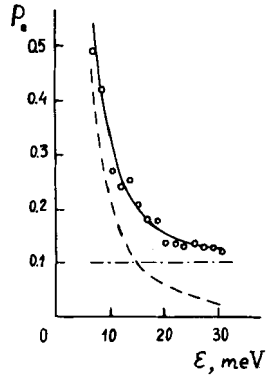

FIGURE 7 The dependence of the electron diffusion coefficient on the energy.

c) *Photon Drag Effect on Interband Optical Transitions in GaAs. Resonance Recoil During Optical Phonon Emission*

During the light absorption on interband optical transitions an electron and hole are excited with the total momentum q. Moreover, an average momentum belongs to electron and hole are equal, respectively[17] to: $\mathbf{q}_e = \mathbf{q}m_e/(m_e + m_h)$, $\mathbf{q}_h = \mathbf{q}m_h/(m_e + m_h)$. Neglecting photoexcitation the anisotropy of the photoexcited electrons is distributed uniformly on the sphere in the momentum space displaced on the vector $\mathbf{q}_e$ from the center (Figure 8). The PDE is composed for this from two effects: (1) an average electron velocity on the displaced sphere, (2) dependence of the momentum relaxation time on the electron energy. The electrons possess the relaxation time of $\tau_- = \tau(E - \mathbf{k}\mathbf{q}_e/m_e)$ in the left part of the sphere and the relaxation time of $\tau_+ = \tau(E + \mathbf{k}\mathbf{q}_e/m_e)$ in the right part of the sphere. Consequently, even with equal electron velocities in the left and right parts of the sphere k/m_e the currents from the left and right halfspheres do not compensate for each other because of the difference τ_+ and τ_-. To separate the V_{SPG} contribution from the general signal the emf difference for two equal in the magnitude, but opposite in the sign of the incident angle θ was measured in the perpendicular to the incident plane polarization. The emf V_{SPG} is absent and V_0 is excluded by subtraction in this geometry. The experimental PDE spectrum is represented by the point in Figure 9. One can see that the spectrum consists of signchangable oscillations caused by the step electron isotropization according to the scattering during the LO-phonon emission. The

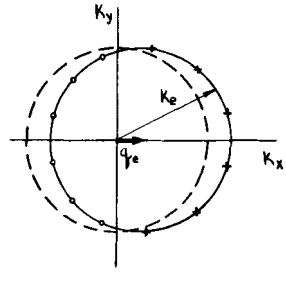

FIGURE 8 The obvious explanation of the nature of the PDE photocurrent and the resonance recoil effect. The solid line marks the sphere of the electron photoexcitation with the account of the photon momentum. The dotted line represents the sphere of the constant energy (the boundary of the passive band).

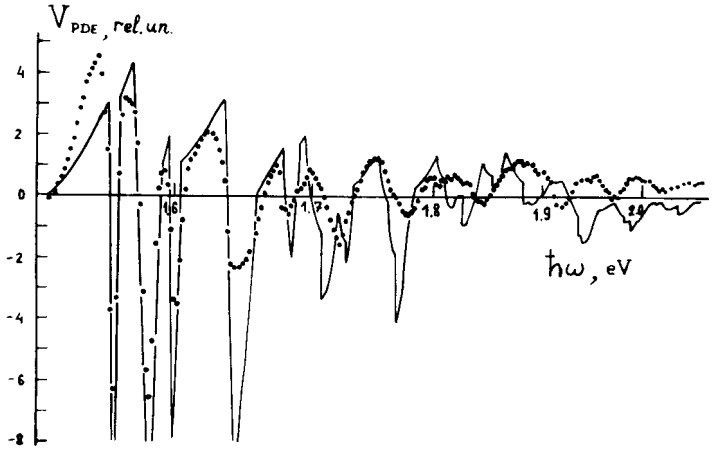

FIGURE 9 The photon drag effect spectrum in the specimen. The solid line is theory, the points represent the experiment.

sign of positive oscillations corresponds to the electron stream along the photon momentum $\mathbf{q}$. Unlike the SPG the contributions to the SPG from the electrons excited in light and heavy channels have the same signs. There are narrow negative peaks on the thresholds of the electrons of *LO*-phonons emitting, which correspond to an electron stream in the direction opposite to the photon momentum $\mathbf{q}$ (the resonance recoil effect).[16,17] The hole resonance peaks which must be positive do not appear in the experimental spectrum. A vivid explanation of the resonance recoil peaks is illustrated in Figure 9. The dotted line limits the region in the $\mathbf{k}$-space where electron energy E is less than $\hbar\Omega_{LO}$ (the passive band). The sphere section in which the photoexcited electrons are distributed is shown with a solid line. The sphere center is displaced from the point $\mathbf{k} = 0$ on the momentum $\mathbf{q}_e = \mathbf{q}m_e/(m_e + m_h)$ due to the finiteness of the photon momentum $\mathbf{q}$. In the resonance region this sphere intersects the boundary of the passive band. One can see that the electrons moving along the photon momentum (a circle part marked by crosses) have the energy of $E > \hbar\Omega_{LO}$. These electrons, for the time $\tau = 5 \cdot 10^{-13}$ sec of *LO*-phonon emitting fall quickly on the conducting band bottom and do not give contribution in the photocurrent. The sign and magnitude of the photocurrent are determined by the electrons moving opposite to the momentum $\mathbf{q}$, which are in the passive band and have a large free path length.

The theoretical photocurrent spectrum computer calculated is shown in Figure 9 with a solid line. The same values of the GaAs band structure parameters and the same scattering mechanisms as for the SPG calculation were used. The theory gives the correct order of the photocurrent magnitude, describes well the position of the oscillation peaks up to the frequency of $\hbar\omega \sim 1.8 + 1.9$ ev, where the excitation of spin splitting holes and electron scattering in the side minimum of the conduction band take place. However, in the oscillation form there is essential difference with the experiment. The hole contribution to photocurrent is found less essential than the electron contribution due to a stronger hole scattering on the acoustic phonons.

The first recoil peak measured with greater precision than the spectrum in Figure 8 on two specimens with similar parameters is represented in Figure 10. Its integral intensity normalized on the photocurrent maximum at frequency $\hbar\omega \sim 1.55$ ev is equal to $\sim 0.5\ \Omega_{LO}$ what is close to the theoretical value of $0.7\ \Omega_{LO}$ calculated on the base of formula (16). The experimental peak width is 5 mev, the broadenings due to the finiteness of the photon momentums[16,17] and those due to the goferness of the hole dispersion lows are, respectively 2 and 1 mev. The remaining 2 mev are apparently connected with nonhomogeneous and device broadening. The recoil peak width on the theoretical spectrum (Figure 8) was calculated as the sum of the widths due to all these mechanisms, the integral intensity of the peaks corresponded to formula (16), the peak form was

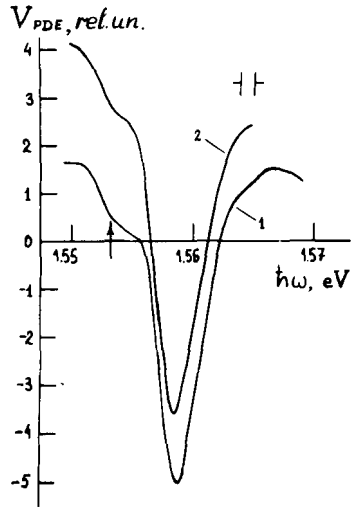

FIGURE 10 The first recoil pick in the specimen S52 shown by curve 1, and in the specimen S57 ($\mu = 10^5$ cm^2/v sec, $n = 10^{14}$ cm^{-3}) is represented by curve 2. Curve 2 is displaced by one unit upwards for clearity.

chosen parabolic because a precise form is rather complicated. The "shoulder" on the left side of the recoil peak situated at the distance of 5 mev from the peak center and shown with an arrow in Figure 10, is caused, apparently, by the process of electron capture on the shallow donor with *LO*-phonon emission. The PDE measurement is actually a differential methodics because in formula (15) there are terms with the energy derivative $\partial\Lambda(E)/\partial E$. This circumstance gives the possibility to reveal a delicate spectral peculiarity which was not observed in the photoemf and SPG spectrums.[6,29]

d) *The Bulk Photogalvanic Effect on Interband Transitions in GaAs*

The origin of the bulk PGE on the interband optical transitions is the probability asymmetry of electron and hole photoexcitation which is not connected with the photon momentum **q**. For a particular direction in the momentum space the electrons with momentum **k** and the holes with momentum $-\mathbf{k}$ with direct optical transition are photoexcited to a greater extent than the electrons with momentum $-\mathbf{k}$ and holes with momentum **k**. In the goferness neglection the electrons and holes excited by the light are distributed asymmetrically on the sphere in the momentum space with the center at the Brillouin band center. They give the contributions in the photocurrent of the same sign.

Here we give the results of the preliminary experiment and the measurement of the bulk PGE in GaAs. The photovoltage V_{PGE} was measured with normal incidence of the light on the specimen with orientation (110). In experiment geometry the SPG and PDE do not give contribution to the photocurrent along the specimen surface. The contacts were parallel to the direction (1, $\bar{1}$, 1). In that case V_{SPG} depends in the following manner on the angle φ between the light vector of polarization and the current propagation direction (1, $\bar{1}$, $\bar{2}$)

$$V_{SPG}(\varphi) = \frac{\sqrt{2}\, n_\omega I \beta_\omega R}{(1+n_\omega)^2}\left[\frac{1}{\sqrt{3}} + \cos(\psi + 2\varphi)\right] \tag{24}$$

Here n_ω is the GaAs refractive index; β_ω is a photogalvanic constant, defined by relation (2), R total specimen resistance, $\cos\psi = 1/\sqrt{3}$. The photovoltage V_{PGE} equal to the difference between the maximum and minimum, with respect to angle φ, emf values was determined experimentally. The V_{PGE} spectrum is shown in Figure 11. According to the qualitative arguments discussed above the experimental curve V_{SPG} contains definite sign oscillations with characteristic steps on the thresholds of the *LO*-phonons emission. Note, that the experimental precision of the PGE distinguishing is less than for SPG and PGE due to its relative smallness. Therefore, the agreement between theoretical curve (14) and experimental data have to a great extent a qualitative character. From the comparison of the theory and experiment we estimate the photogalvanic constants $\beta(\omega) = 10^{-2}$

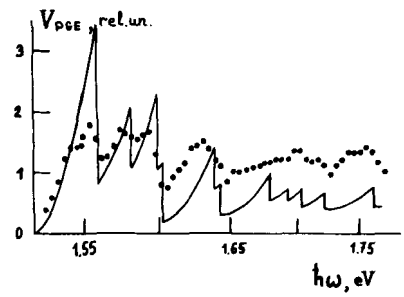

FIGURE 11 The spectrum of the bulk photogalvanic effect. The solid line is theory, the points represent the experiment.

Am/wt at the frequency of $\hbar\omega = 1.556$ ev and the λ constant that characterizes the Kane Hamiltonian asymmetry $\lambda = 0.1\ m_0^{-1}$.

CONCLUSION

The theory of the photogalvanic effects on interband optical transitions developed in the present paper sufficiently well describes the basic spectral peculiarity of the surface photogalvanic effect, photon drag effect and bulk photogalvanic effect investigated experimentally in gallium arsenide. The spectra of photogalvanic effects contain detailed information about the processes of momentum relaxation of the charge carriers. Especially rich information one can obtain from the measurement of photogalvanic effect spectra in the magnetic field, that give a possibility to determine directly the energy dependence of electron frequency collisions according to the momentum. Undoubtedly that further development of the experimental investigation of the photogalvanic effects spectra will give the possibility to obtain extensive and detailed information about the processes of momentum relaxation in the volume and surface of solid bodies.

REFERENCES

1. S. M. Rivkin. Photoelectric phenomena in the semiconductors, Moscow, Fismatgiz, (1963).
2. V. I. Belinicher and B. I. Sturman. *Uspekhi Fizicheskich Nauk*, **130,** 415 (1980).
3. V. M. Fridkin and B. N. Popov, *ibidem*, **126,** 657 (1978).
4. A. M. Danishevsky, A. A. Kastalsky, S. M. Rivkin and I. D. Jaroshezky, *JETP*, **58,** 544 1970; A. A. Greenberg, *JETP*, **58,** 989 (1970).
5. L. I. Magarill and M. V. Entin, *FTT*, **21,** 1280 (1979).
6. V. L. Alperovich, V. I. Belinicher, V. N. Novikov and A. S. Terekhov, *Pis'ma JETP*, **31,** 581 (1980); *JETP*, **80,** 2298 (1981).
7. Ju. S. Galpern and Sh. M. Kogan, *JETP*, **56,** 35 (1969).
8. V. I. Belinicher and S. M. Rivkin, *JETP*, **81,** 353 (1981).
9. A. M. Dichne, V. A. Rosljakov and A. H. Starostin, *Dokladi AN SSSR*, **254,** 599 (1980).
10. V. I. Belinicher and V. N. Novikov, *Fiz. Techn. Polup.*, **15,** 1957 (1981).
11. G. L. Bir and G. E. Pikus, Symmetry and deformation effects in the semiconductors, Moscow, Nauka (1972).
12. M. I. Djakonov and V. I. Perel, *JETP*, **60,** 1954 (1971).
13. V. I. Belinicher: *FTT*, **23,** 1980 (in press).
14. V. I. Belinicher and V. N. Novikov, Preprint N 153 IAiE SO AN SSSR (1981).
15. V. D. Dimnikov, M. I. Djakonov and V. I. Perel, *JETP*, **71,** 2373 (1976).
16. A. A. Greenberg and L. V. Udod, *Fiz. Techn. Polup.*, **8,** 1012 (1974).
17. A. A. Greenberg, D. S. Buljaniza and Z. Z. Imamov, *Fiz. Techn. Polup.*, **7,** 45 (1973).
18. A. F. Gibson and A. P. Serafetinides, *J. Phys.*, **C8,** 3147 (1975).
19. V. L. Alperovich, V. I. Belinicher, V. N. Novikov and A. S. Terekhov, *Pis'ma JETP*, **33,** 573 (1981).
20. B. P. Zacharchenja, V. I. Zemsky and D. N. Mirlin, *Pis'ma JETP*, **24,** 96 (1976).
21. V. I. Okulov and V. V. Ustinov, *Fiz. Nizk. Temp.*, **5,** 213 (1979).
22. I. M. Zidelkovsky, Band structure of semiconductors, Moscow, Nauka (1978).
23. D. N. Mirlin, L. P. Nikitin, I. I. Reshina and V. F. Sapega, *Pis'ma JETP*, **30,** 419 (1979).
24. V. D. Dimnikov, *JETP*, **77,** 1107 (1979).
25. A. P. Levanjuk, A. R. Rogosjan and E. M. Ujukun, *Dokladi AN SSSR*, **256,** 60 (1981).
26. B. N. Popov and V. N. Fridkin, *ibidem*, **256,** 63 (1981).
27. V. L. Alperovich, A. F. Kravchenko, N. A. Pachanov and A. S. Terechov, *Pis'ma JETP*, **28,** 551 (1978).
28. D. N. Mirlin, I. Ja. Karlik, L. N. Nikitin, I. I. Reshina and V. F. Sapega, *Pis'ma JETP*, **32,** 34 (1980).
29. V. L. Alperovich, A. F. Kravchenko, N. A. Pachanov and A. S. Terekhov, *Fiz. Techn. Polup.*, **14,** 1768 (1980).